Liposome accumulation in irradiated tumors display important tumor and dose dependent differences

Hansen, Anders Elias; Fliedner, Frederikke Petrine; Henriksen, Jonas Rosager; Jørgensen, Jesper Tranekjær; Clemmensen, Andreas Ettrup; Børresen, Betina; Elema, Dennis Ringkjøbing; Kjær, Andreas ; Andresen, Thomas Lars

Published in:
Nanomedicine: Nanotechnology, Biology and Medicine

Link to article, DOI:
10.1016/j.nano.2017.08.013

Publication date:
2018

Document Version
Peer reviewed version

ELSEVIER
Nanomedicine: Nanotechnology, Biology, and Medicine
xx (2017) xxx–xxx
nanomedicine
Nanotechnology, Biology, and Medicine
nanomedjournal.com

Liposome accumulation in irradiated tumors display important tumor and dose dependent differences

Anders Elias Hansen, DVM, PhD[a,b,c,1], Frederikke Petrine Fliedner, MSc[b,c,1], Jonas Rosager Henriksen, MSc, PhD[b,d], Jesper Tranekjær Jørgensen, MSc, PhD[c], Andreas Ettrup Clemmensen, MSc[c], Betina Børresen, DVM[a,e], Dennis Ringkjøbing Elema, MSc, PhD[f], Andreas Kjær, MD, DMSc, PhD[c], Thomas Lars Andresen, MSc, PhD, Prof[a,b,*]

[a]*Department of Micro- and Nanotechnology, DTU Nanotech, Technical University of Denmark, Kongens Lyngby, Denmark*
[b]*Center for Nanomedicine and Theranostics, Technical University of Denmark, Kongens Lyngby, Denmark*
[c]*Department of Clinical Physiology, Nuclear Medicine & PET and Cluster for Molecular Imaging, Department of Biomedical Sciences, Rigshospitalet and University of Copenhagen, Copenhagen, Denmark*
[d]*Department of Chemistry, DTU Chemistry, Technical University of Denmark, Kongens Lyngby, Denmark*
[e]*Department of Small Animal Clinical Sciences, Copenhagen University, Frederiksberg, Denmark*
[f]*Hevesy Laboratory, DTU Nutech, Technical University of Denmark, Roskilde, Denmark*

Received 29 March 2016; accepted 21 August 2017

Abstract

Radiation therapy may affect several important parameters in the tumor microenvironment and thereby influence the accumulation of liposomes by the enhanced permeability and retention (EPR)-effect. Here we investigate the effect of single dose radiation therapy on liposome tumor accumulation by PET/CT imaging using radiolabeled liposomes. Head and neck cancer xenografts (FaDu) and syngenic colorectal (CT26) cancer models were investigated. Radiotherapy displayed opposite effects in the two models. FaDu tumors displayed increased mean accumulation of liposomes for radiation doses up to 10 Gy, whereas CT26 tumors displayed a tendency for decreased accumulation. Tumor hypoxia was found negatively correlated to microregional distribution of liposomes. However, liposome distribution in relation to hypoxia was improved at lower radiation doses. The study reveals that the heterogeneity in liposome tumor accumulation between tumors and different radiation protocols are important factors that need to be taken into consideration to achieve optimal effect of liposome based radio-sensitizer therapy.

Key words: Liposome; PET; Radiotherapy; Radio-sensitizer; Hypoxia

External beam radiation therapy (RT) is a central part of the treatment regimen for more than half of all cancer patients. Liposomal drug delivery systems that carry radio-senzitizers to tumors can potentially improve therapeutic efficacy of RT without increasing loco-regional side effects in the irradiated region.[1,2] Combining targeted RT and targeted drug delivery can therefore increase regional tumor control.[3] Moreover, liposomes are flexible in regards to the selection of drugs that can be encapsulated, transported and released within tumors. Liposomes can therefore serve as optimal delivery systems for targeting radiosensitizers to malignant tissue.[1,2] However, liposome accumulation in solid tumors has been demonstrated to depend on multiple factors, including interstitial pressure, tumor vasculature and perfusion.[4–6] Liposome extravasation by the enhanced permeability and retention (EPR) effect is primarily driven by transvascular convection and their accumulation is

Conflict of interest: There are no conflicts of interest.

Funding: The support from the European Research Council, the Novo Nordisk Foundation, the Lundbeck Foundation, the Innovation Fund Denmark, the Research Council of Independent Research, the Svend Andersen Foundation and the Arvid Nilsson Foundation is gratefully acknowledged.

*Corresponding author at: Department of Micro- and Nanotechnology, Building 345Ø, room 050, DK-2800 Kongens Lyngby.
E-mail address: thomas.andresen@nanotech.dtu.dk (T.L. Andresen).
[1] These Authors contributed equally to this work.

http://dx.doi.org/10.1016/j.nano.2017.08.013
1549-9634/

inversely correlated to interstitial fluid pressure (IFP) and directly correlated to regional blood perfusion and leakiness.[4,6–8] RT influences these parameters; however, results on the effect on tumor accumulation levels of nano-sized particles are not clear.[6]

Molecular oxygen is the most important radio-sensitizer and hypoxic tumor cells are highly radio-resistant and display increased malignancy. Tumor hypoxia is generally divided in acute perfusion limited, chronic diffusion limited and anemic hypoxic.[9] The nature of tumor hypoxia is closely related to vascular parameters and liposomes may therefore distribute poorly to hypoxic regions. In both experimental and clinical tumors the IFP is increased and associated with an increased malignant phenotype.[10,11] RT has been associated with increased vascular leakiness, and high total radiation doses can potentially increase the extravasation of macromolecules.[6] Pretreating tumors with cytotoxic agents has been identified to increase tumor blood flow and decrease IFP, potentially being the results of a reduction in tumor cell density to alleviate tumor blood vessels compressions and increase the vascular surface area which subsequently increases liposome accumulation.[12,13] Following these observations the effects of RT could also mediate a beneficial effect for macromolecular extravasation by reducing cell density.[11,14] Importantly, single radiation doses >10 Gy, are known to cause significant damage to neoangiogenic tumor vasculature and increase hypoxia and mediate significant secondary cancer cell death following vascular damage.[15] On the contrary, single doses <10 Gy cause mild vascular damage and may potentially increase vascular perfusion and thereby decrease hypoxia after irradiation.[15–17] Few studies of the effect of RT on liposome uptake have been conducted. Single-fraction irradiation had no effect on liposome uptake in human KB cancer xenografts when evaluated by gamma counting radiolabeled liposomes.[18] Considering this and that important tumor dependent differences and responses may exist, we investigated the effect of single fraction radiation therapy on liposome accumulation. This was evaluated by non-invasive PET imaging in regard to i) the potential for improving liposomal drug delivery by RT 24 h prior to liposome administration, ii) the influence of RT on vascular tumor parameters, cellular density and necrosis and iii) locoregional liposome accumulation in hypoxic tumor regions, in a human head and neck cancer xenograft model and in a syngenic murine colon cancer model.

Methods

Tumor model

FaDu (human head and neck cancer) xenografts were established by subcutaneous injection of ~5×10^6 cells suspended in 100 μl of culture medium and Matrigel over the thigh/flank of 7 weeks old female NMRI nude mice. Tumors were allowed to grow for 12-14 days. CT26 (murine colon cancer) syngenic tumors were established by subcutaneous injection of ~3×10^5 cells suspended in 100 μl of culture medium over the thigh/flank of 6 weeks old female Balb/c mice. Tumors were allowed to grow for 18 days. The National Animal Experiments Inspectorate approved all study procedures.

Radiolabeled liposomes

Pegylated liposomes consisting of HSPC:CHOL:DSPE-PEG2k (56.5:38.2:5.3) were remote loaded with the PET isotope $^{64}Cu^{2+}$. Briefly, 100 nm 50 mM pegylated liposomes entrapping 10 mM DOTA were prepared as previously described.[19] Radiolabelling was achieved by adding a volume of liposomes to dried $^{64}CuCl_2$ followed by incubation at 55 °C for 75 min. The loading efficiency was afterward evaluated by Thin Layer Chromatography (Radio-TLC) and Size Exclusion Chromatography (Radio-SEC),[19] which showed a loading efficiency of >98% for both techniques. The liposomes were prepared at either 3.3 mM or 6.6 mM lipid concentration and an activity concentration of 62.5 MBq/ml or 125 MBq/ml (activity at the time of injection) for the FaDu and CT26 tumors respectively. Each animal was dosed with a volume corresponding to 22 μmol/kg and an activity of ~12.5 MBq/animal.

Radiation therapy

Mice carrying FaDu xenografts were randomized into four treatment groups; non-irradiated controls (n = 11), 5 Gy (n = 11), 10 Gy (n = 10) and 20 Gy (n = 11). Mice carrying CT26 tumors were randomized into four treatment groups; non-irradiated controls (n = 8), 2 Gy (n = 8), 5 Gy (n = 8) and 10 Gy (n = 8). Radiation therapy was delivered as a single fraction at a dose-rate of 1 Gy/min (320 kV, 12.5 mA) using a small animal irradiator (X-rad320, pXi, CT, USA). Mice were irradiated in a dedicated fixation device securing that only the tumor bearing leg was exposed to irradiation and the remaining body shielded.

MicroPET/CT imaging

PET/CT imaging was performed on an Inveon® small animal PET/CT system (Siemens Medical Systems, PA, USA) approximately 24 h after completion of RT. Mice were anesthetized by inhalation anesthesia (~3% sevoflurane) and ^{64}Cu-liposomes injected into a tail vein. ^{64}Cu-liposomes were allowed to distribute for 1 h before commencing a 5-min PET scan (1-h scan) followed by a corresponding CT scan. A similar PET/CT scan (15 min acquisition) was performed after a distribution period of 24 h (24-h scan). Emission data were corrected for dead time and decay and attenuation correction was performed based on the corresponding CT scan. PET scans were reconstructed using a maximum a posteriori (MAP) reconstruction algorithm (0.815 × 0.815 × 0.796 mm). Image analysis was performed using Inveon® software (Siemens Medical Systems, PA, USA). 3D regions of interest (ROIs) were manually constructed and decay corrected data (%injected dose per gram tissue (%ID/g)) reported.

Immunohistochemistry CD31, cell density and necrosis

Immunohistochemistry (IHC) was performed on formalin-fixed, paraffin-embedded 4 μm tumor sections that were stained with H&E for histological evaluation and with CD31 antibodies for tumor blood vessels. CD31 staining was performed by

heating sections at 60 °C (1 h) followed by deparaffination in xylene and rehydration. Antigen retrieval was performed by microwave-based antigen retrieval. Endogeneous peroxidase was blocked using peroxidase blocking reagent (Dako, Glostrup, Denmark) for 8 min and sections blocked in 2% BSA for (10 min). Sections were incubated with primary CD31 antibody (Abcam, diluted 1:100) in 2% BSA (1.5 h/room temperature) followed by incubation with secondary biotinylated EnVision FLEX™ (40 min) (Dako, Glostrup, Denmark). Tissue sections were stained with DAB (10 min) and counterstained with hematoxylin. Between all steps sections were rinsed in PBS.

Slides were mounted for electronic slide scanning (Axio scan, Carl Zeiss, Germany) (pixel size 0.022 × 0.022 μm). Tumor necrosis was evaluated using the Advanced Weka segmentation plug-in for Fiji (ImageJ). The degree of necrosis in sections was determined by drawing ROIs in necrotic, background/artifacts and viable tumor region and transferring these to the trainable classifier to determine necrotic and viable areas.

Ten regions were selected on CD31 stained sections and sent for analysis of microvessel density by automated segmentation algorithm for analysis of microvessels in immunostained histological tumor sections (CAncer IMage ANalysis: http://www.caiman.org.uk).[20,21] The regions were additionally transferred to Fiji (ImageJ) for determination of nuclear density. In short, color deconvolution was performed to yield a separate hematoxylin image and the nuclei density determined by excluding fragments and artifacts by automated exclusion of structures below a cut-off size of (50 pixels^2).

^{64}Cu-liposome autoradiography and hypoxia immunohistochemistry

For analysis of intratumoral distribution of liposomes and hypoxia FaDu tumors (controls) were intravenously injected with the radiolabeled liposomes and these were allowed to distribute for 24 h before sacrificing and bleeding mice. To further study the influence of radiation therapy on intratumoral hypoxia and liposome distribution, tumors from and two CT26 tumors from each group were subjected to autoradiography and hypoxia immunohistochemistry (26 h distribution period for liposomes). For hypoxia immunohistochemistry the exogenous hypoxia marker Pimonidazole (60 mg (kg animal)$^{-1}$ in PBS), was administered by intraperitoneal injection two hours before sacrifice. After sacrificing and bleeding animals, tumors were snap frozen and cryosectioned (8 μm) in cutting media. Sections separated by at least 400 μm were thaw mounted on Superfrost Plus microscopy slides. Seventeen sections from eight different FaDu tumors and five sections from included CT26 tumors were evaluated. Intratumoral distribution of ^{64}Cu-liposomes was determined by exposing tumor sections to phosphor imaging screens for approximately 18 h (−20 °C). Phosphor screen was read using a phosphor imaging system (Cyclone Plus, Perkin Elmer, MA, USA) and semi-quantitative luminescence images (pixel size 0.04 × 0.04 mm) were obtained.

Tumor sections were fixed in acetone (4 °C/10 min). Tissue peroxidase was quenched using peroxidase blocker (Dako, Glostrup, Denmark) and non-specific binding blocked using 2% BSA. Pimonidazole immunohistochemistry was performed using mouse monoclonal anti-pimonidazole antibody (Hypoxyprobe, MA, USA) diluted in 2% BSA (1:600) (1 h) followed by Secondary biotinylated anti-mouse antibody (40 min) (Envision Flex, Dako, Glostrup, Denmark). Antibody binding was visualized using DAB and sections were counterstained with hematoxylin (H) and slide scanned as described above.

ROIs, including viable tumor regions and excluding necrotic regions and artifacts were manually drawn (Fiji, ImageJ, NIH, MD, USA). Automated DAB-H color deconvolution and manual thresholding of pimonidazole IHC staining followed by image binarization was performed in Fiji software. Autoradiography images were co-registered to the corresponding pimonidazole DAB-H images using a rigid co-registration algorithm (MATLAB 8.4, The MathWorks, Inc., MA, United States). Pimonidazole values on rescaled image (autoradiopgraphy resolution) represent mean level pimonidazole positive pixels on the constructed binarized image. ^{64}Cu-liposome autoradiography pixels were categorized into four activity levels (0-0.25, 0.26-0.50, 0.51-0.75 and 0.76-1.0) relative to the individual slide single pixel maximum. The corresponding mean pimonidazole pixel values for the four ^{64}Cu-Liposome categories were determined for each slide and bar-plots constructed.

Statistical analysis

Prism 7 (GraphPad Software, La Jolla, CA., USA) was used for all statistical analysis. One-way or two-way ANOVA analysis and Holm–Sidak multiple comparison test were applied for comparisons of groups. All data are reported as mean ± SEM (standard error of mean) unless otherwise stated and a P-value <0.05 considered statistically significant.

Results

^{64}Cu-liposome PET/CT after radiation therapy

Radiation therapy was successfully delivered to all mice 24 h before administration of radiolabeled liposomes. The treatment schedule was chosen to ensure that the acute effect of irradiation was activity during the period of liposome distribution. To evaluate the effects of the different radiation doses we extracted tumor activity levels of ^{64}Cu-liposome PET data from the co-registered PET/CT images from the 1-h and 24-h PET/CT scans. Two PET scans were performed to extract information on accumulation, as intravascular liposome activity is expected to dominate the 1-h PET scan and liposomes that have extravasated through fenestrated tumor blood vessels the 24-h scan. PET/CT images from the 24-h scans from each treatment group are illustrated in Figure 1, *A-H*.

FaDu tumors displayed no significant ^{64}Cu-liposome activity difference between controls and treatment groups at the 1-h PET/CT (Figure 2, *A* and *B*). At the 24-h PET/CT FaDu tumors receiving 5 Gy and 10 Gy had significantly higher mean liposome activity compared to the control group, while no statistical difference was observed for the mean activity of the 20 Gy treatment group (Figure 2, *C*). For the comparison of the 24-h maximum activity, only the 5 Gy treatment group was statistically higher than the control group (Figure 2, *D*). The

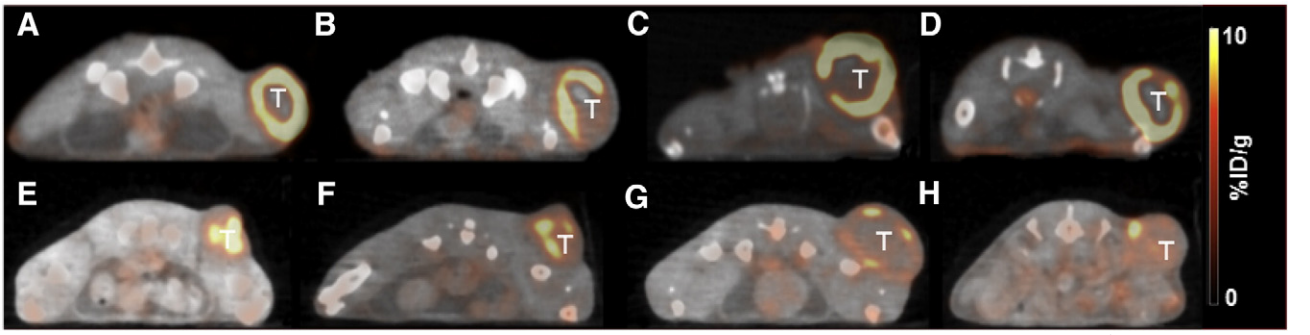

Figure 1. ^{64}Cu-liposome PET/CT of FaDu xenografts (top row) **(A)** non-irradiated control (n = 11), **(B)** 5 Gy (n = 11), **(C)** 10 Gy (n = 10), **(D)** 20Gy (n = 11)) and CT26 tumors (bottom row) **(E)** non-irradiated control (n = 8), **(F)** 2 Gy (n = 8), **(G)** 5 Gy (n = 8), **(H)** 20 Gy (n = 8). (T) Tumor.

influence of radiation on liposome accumulation was further investigated in the syngenic CT26 tumors. Following the higher radiosensitivity in comparison to FaDu tumors, an irradiation schedule of 2 Gy, 5 Gy and 10 Gy was chosen. Interestingly, for the CT26 tumors an inverse correlation between radiation dose and liposome accumulation was observed. There was significantly higher mean activity of liposomes in the control group compared to all treatment groups at the 1-h PET scan (Figure 2, *E*). The control group also displayed the highest maximum activity of ^{64}Cu-liposomes at the 1-h scan although this was not significant in comparison to irradiated groups (Figure 2, *F*). These observations could indicate that a high level of damage was induced to intratumoral blood vessels that limit intravascular liposome blood activity. Opposite to the observations in FaDu tumors, the irradiated CT26 groups displayed lower activity levels in comparison to controls. This was however only statistically significant for the controls in comparison to the 5 Gy irradiated group (Figure 2, *G* and *H*). Based on the conflicting results of the liposome uptake in the two included tumor models we evaluated the effect of radiation dose on tumor parameters that are expected to influence liposome accumulation.

Micro vessels, nuclear density and necrosis

The levels of intratumoral necrosis, nuclear density and micro vessels were investigated on stained tumor sections. For the FaDu tumor we observed a higher level of intratumoral necrosis primarily in the central parts of the tumors whereas less and more scattered distribution of necrosis was observed for the CT26 tumors. FaDu non-irradiated controls displayed a mean intratumoral necrosis level of 21.6% (± 4.5) while CT26 tumors only displayed 11.0% (± 1.3). For both tumor types the level of intratumoral necrosis increased with higher doses of radiation, except for the comparison of the 5 Gy FaDu group and controls. However, only the 20 Gy FaDu group and the 5 Gy and 10 Gy CT26 groups and corresponding controls were significantly different (Figure 3, *A* and *D*). As liposome accumulation is not expected to occur in devascularized non-vital necrotic regions this could explain the observed lower activity in comparison to controls for the 20 Gy FaDu group and the irradiated groups of CT26 tumors.

Nuclear density was found to decrease with increasing radiation dose. The cell density in the treatment groups all, except for the 5 Gy FaDu group, displayed significantly lower cellular density compared to control groups for both tumor types (Figure 3, *B* and *E*). The lower cell density is expected to decrease interstitial pressure in tumors and therefore facilitate an easier extravasation of liposomes. However, this was correlated to an increased the overall ^{64}Cu-liposome accumulation. Additionally, cell density could potentially be counteracted by pressure changes stimulated by radiation-induced inflammation, apoptosis, necrosis and acute microvessel damage.

The micro vessel density (MVD) was investigated to identify if blood vessel density could explain the observed liposome activity differences. The MVD displayed no significant difference between FaDu groups (Figure 3, *C*). Interestingly, the CT26 control group displayed significantly higher MVD than all irradiated groups (Figure 3, *F*). The higher mean ^{64}Cu-liposome activity at the 1-h PET could potentially be explained by the higher microvessel density. However, for the 24-h scan this did not result in significantly higher activity, whereas the FaDu tumors displayed significantly higher activity levels for the 5 Gy and 10 Gy groups.

Microregional distribution of ^{64}Cu-liposomes and pimonidazole

To investigate the potential of liposomal drug delivery system to improve therapeutic control of radio-resistant hypoxic tumor regions we compared the accumulation of radiolabeled liposomes to pimonidazole hypoxia immunohistochemistry. ^{64}Cu-liposome autoradiographies were compared to of pimonidazole immunohistochemistry for non-irradiated FaDu tumor sections. The co-registration process and resizing of images allowed us to include seventeen sections in the analysis. The microregional pixel-to-pixel comparison of pimonidazole values and corresponding categorized ^{64}Cu-liposome activity level identified that hypoxia decreases significantly with increasing (within slide) ^{64}Cu-liposome activity (Figure 4, *A-D*). This observation is important for liposome based radiosensitizer therapy, as they may have limited access to important hypoxic regions at least for the liposomes under investigation. Following the observed influence of radiation cellular density and vascular function the influence of dose on pimonidazole positive fraction was investigated in CT26 tumors. We observed a significantly

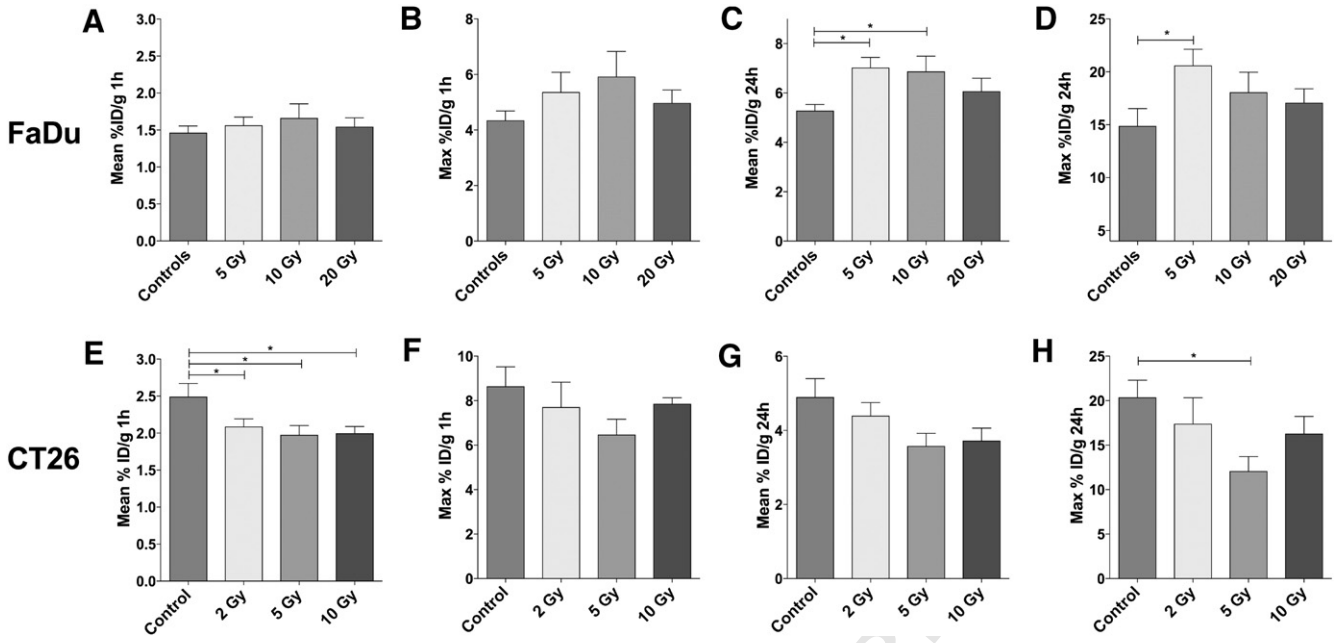

Figure 2. Tumor mean and maximum activity levels at 1-h and 24-h after injection of ^{64}Cu-liposomes evaluated by PET/CT for control and treatment groups. FaDu tumors **(A-D)** and CT26 tumors **(E-H)** (%ID/g ± SEM) (*$P < 0.05$).

lower fraction of pimonidazole positive pixel in the 2 Gy irradiated group, no difference for the 5 Gy group and a significantly increased positive fraction in the 10 Gy group relative to controls (Figure 4, *E*). To determine if the observed changes in tumor oxygenation could influence the distribution patterns of liposomes relative to microregional hypoxia a comparison of ^{64}Cu-liposome activity level and pimonidazole was performed. The control group displayed an inverse correlation that was comparable to that of non-irradiated FaDu tumors (Figure 4, *F*). However, the 2 Gy and 5 Gy irradiated groups displayed an almost similar level of hypoxia in the different levels of ^{64}Cu-liposome activity, which could indicate that these dose ranges can potentially both decrease levels of hypoxia and improve liposome accumulation in regards to hypoxic areas. This must of course be weighed against the overall accumulation of ^{64}Cu-liposomes.

Discussion

The therapeutic combination of tumor targeting liposome-encapsulated radiosensitizers and radiation therapy holds great clinical potential following the dual tumor targeting properties. Notwithstanding this potential, the direct link between the parameters of central importance for liposome accumulation and the effects of radiation therapy makes the determination of optimal timing of radiation and dose and liposome administration important.

The two cancer models yielded opposite results in respect to liposomes accumulation. Whereas radiation improved accumulation in FaDu xenografts after 24-h (5 Gy and 10 Gy groups), the CT26 tumors displayed an insignificant decrease in liposome accumulation after radiation. These observations are interesting in respect to the study in human KB cancer xenografts where no effect, negative or positive, on liposome uptake was observed for radiation doses from 5 to 20 Gy evaluated invasively from 1 to 96 h after irradiation.[18] Both cancer models displayed an increase in intratumoral necrosis and decreased cell density following irradiation, both of which were most significant for the CT26 tumors. Interestingly, MVD was found to respond very differently to irradiation between the models. Irradiation significantly decreased MVD in CT26 while FaDu tumors did not display changes or patterns in relation to radiation. This was also illustrated by the mean ^{64}Cu-liposome activity between groups after a circulation period of only 1-h. In clinical head and neck squamous cell carcinomas a decrease in MVD was correlated to an improved response and overall survival.[17] In light of this, our results indicate that the FaDu tumors represent a more radio-resistant tumor and that adjuvant liposomal radiosensitizer therapy could be beneficial, at least from a dose accumulation perspective for tumors maintaining a high MVD during irradiation. Based on the differences in liposomes accumulation and the histological analysis, accumulation appeared directly dependent on a high MVD. This observation is in agreement with previous publications identifying, blood flow as the rate limiting step for liposome extravasation in tumors with a high vascular permeability.[25] However, irradiation can decrease nuclear density and damage vascular structures to potentially increase liposome accumulation by lowering IFP and facilitating transvascular extravasation. No direct measures for IFP in addition to nuclear density were performed but in a previous report on irradiation of colon carcinoma xenografts single fractions of 10 Gy significantly lowered IFP in tumor.[22] From our results, the differences between MVD response and comparable decrease in nuclear density between FaDu and CT26 tumors indicate that the MVD is the most important parameter to

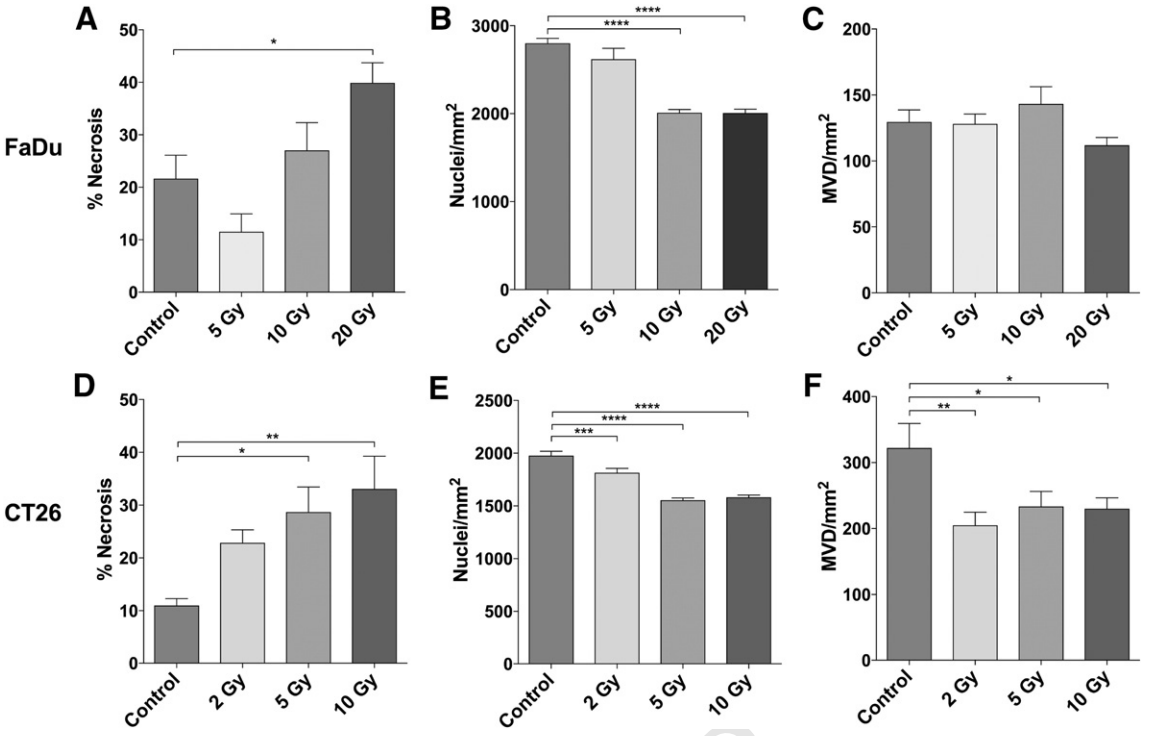

Figure 3. Immunohistochemical analysis of percentage of necrosis, nuclear counts per mm^2 and microvascular density (MVD/mm^2) determined by automated segmentation on tumor sections from control and treatment groups (mean ± SEM). FaDu tumors **(A-C)**. CT26 tumors **(D-F)** (mean ± SEM). *$P \leq 0.02$, **$P \leq 0.005$, ***$P < 0.001$, ****$P < 0.0001$.

influence liposome accumulation. Compatible results were obtained for non-small cell lung cancer patients receiving adjuvant liposomal doxorubicin to fractionated radiotherapy where MVD was associated with increased accumulation and therapeutic efficacy.[23] However, the association of MVD to hypoxia could also influence this observation as discussed below. Interestingly, the increased liposome accumulation for irradiated FaDu tumors could also result from a decreased IFP which may improve tumor perfusion by alleviating pressure dependent collapse of intratumoral vessels.[24,25] Importantly, the optimal timing of liposomal drug administration in relation to fractionated radiation remains to be determined and the reported negative impact of RT five days after irradiation indicates that timing is central for optimization of liposome accumulation.[22] Based on our observations improving liposome accumulation is a balance between maintaining functional blood vessels and improving intratumoral blood flow as discussed in recent literature.[26] However, the heterogeneous response of different tumor models, in regards to these parameters, highlights the value of directly quantitative PET imaging using radiolabeled liposomes.

Single doses of (≥10 Gy) RT induce high levels of vascular damage that leads to secondary cell death when areas become deprived of oxygen and nutrients. On the other hand, fractionated low dose irradiation of tumors has been associated with improved perfusion and reoxygenation.[15–17] The tumor sections evaluated from the 2 Gy and 5 Gy CT26 groups displayed less hypoxia across all levels of liposome activity, which is in line with reports on early reoxygenation after low dose irradiation. This indicates that the low dose irradiation, at least for the CT26 tumors, improves vascular perfusion and tumor oxygenation and provides the basis for a more homogeneous distribution of liposomes. The effect of radiation therapy can therefore potentially also improve liposome penetration and the potential of targeting liposomes that suffers from inability to reach their target if trapped in the perivascular regions.[8] Considering the importance of hypoxia and its intricate link to vascularization, optimized radiation schedules can potentially improve the distribution of liposomes in radioresistant hypoxic region.[25] Liposomal doxorubicin has been reported to increase radiosensitivity in hypoxic prostate cancer xenografts in one study where clamping of the tumor-bearing leg was used to induce hypoxia during RT. However, liposomes were administered prior to clamping and the study therefore provides no evidence that doxorubicin reaches regions of perfusion and diffusion limited hypoxia, but highlights the potential of liposomal chemoradiotherapy.[27] Liposomal doxorubicin and cisplatin, injected 16 h before irradiation, increased the therapeutic efficacy for 4.5 Gy single dose and 9 Gy/3 fractions but not a single dose of 9 Gy radiotherapy in KB head and neck cancer xenografts. No benefit was observed from dosing liposomes as a single compared to multiple injections of the same dose and the authors were not able to determine if the effects observed were truly radiosensitizing or additive,[28] which highlights the importance of timing to achieve a supra-additive effect chemoradiotherapy.

Conclusion

The present study was conducted using a radiolabeled liposome imaging system that provided quantitative data on

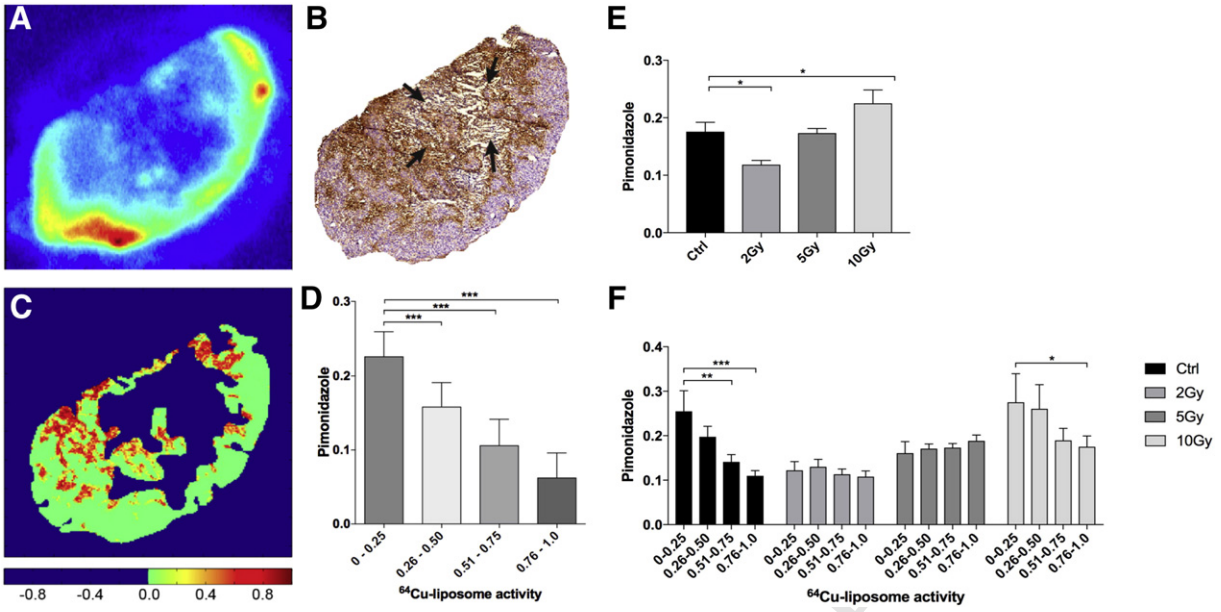

Figure 4. Microregional ^{64}Cu-liposome and pimonidazole distribution evaluated on cryosectioned tumor slides. Illustrative section from a control tumor **(A)** ^{64}Cu-liposome autoradiography, **(B)** pimonidazole peroxidase and hematoxylin (DAB-H) immunohistochemistry, black arrows indicate a central necrotic region, **(C)** interpolated pimonidazole image in false-color, color bar illustrates percent of pimonidazole positive pixels from a constructed binary pimonidazole image. **(D)** Bar plot illustrating the association between regional level of liposome and degree of pimonidazole hypoxia. Pimonidazole pixel values and the corresponding ^{64}Cu-liposome pixel activity levels categorized according to maximum pixel activity on autoradiography (mean ± SEM). **(E)** Percentage of pimonidazole positive pixels (mean ± SEM) in tumor sections from controls and irradiated CT26 tumor sections. **(F)** Bar plots illustrating the association between regional ^{64}Cu-liposome activity relative to section maximum and degree of pimonidazole hypoxia for the different CT26 treatment groups and controls. (*$P < 0.05$, **$P < 0.01$, ***$P < 0.001$).

liposome accumulation as a function of RT. The study identifies that RT may influence the EPR effect and liposome accumulation in a tumor and dose dependent manner. This observation emphasizes that the ^{64}Cu-liposome PET imaging system may provide a theranostic tool to identify patients and treatment combinations and kinetics that may benefit from liposomal drug delivery in relation to radiation therapy. Future studies of liposomal drug delivery systems for radiosensitizers focusing on the correlation between liposome accumulation in tumor tissue as a function of RT and the therapeutic effect induced are highly warranted.

References

1. Petersen AL, Hansen AE, Gabizon A, Andresen TL. Liposome imaging agents in personalized medicine. *Adv Drug Deliv Rev* 2012;**64**:1417-1435.
2. R. I. Jolck, L. N. Feldborg, S. Andersen, S. M. Moghimi and T. L. Andresen, Engineering liposomes and nanoparticles for biological targeting. *Adv Biochem Eng Biotechnol*.125:251–80.
3. Koukourakis MI, Koukouraki S, Giatromanolaki A, Kakolyris S, Georgoulias V, Velidaki A, et al. High intratumoral accumulation of stealth liposomal doxorubicin in sarcomas—rationale for combination with radiotherapy. *Acta Oncol* 2000;**39**:207-211.
4. Li Y, Wang J, Wientjes MG, Au JL. Delivery of nanomedicines to extracellular and intracellular compartments of a solid tumor. *Adv Drug Deliv Rev* 2012;**64**:29-39.
5. Jain RK, Stylianopoulos T. Delivering nanomedicine to solid tumors. *Nat Rev Clin Oncol* 2010;**7**:653-664.
6. Multhoff G, Vaupel P. Radiation-induced changes in microcirculation and interstitial fluid pressure affecting the delivery of macromolecules and nanotherapeutics to tumors. *Front Oncol* 2012;**2**:165.
7. Jain RK. Transport of molecules in the tumor interstitium: a review. *Cancer Res* 1987;**47**:3039-3051.
8. Jain RK, Baxter LT. Mechanisms of heterogeneous distribution of monoclonal antibodies and other macromolecules in tumors: significance of elevated interstitial pressure. *Cancer Res* 1988;**48**:7022-7032.
9. Vaupel P. Hypoxia and aggressive tumor phenotype: implications for therapy and prognosis. *Oncologist* 2008;**13**(Suppl 3):21-26.
10. Yu T, Liu K, Wu Y, Fan J, Chen J, Li C, et al. High interstitial fluid pressure promotes tumor cell proliferation and invasion in oral squamous cell carcinoma. *Int J Mol Med* 2013;**32**:1093-1100.
11. Rofstad EK, Ruud EB, Mathiesen B, Galappathi K. Associations between radiocurability and interstitial fluid pressure in human tumor xenografts without hypoxic tissue. *Clin Cancer Res* 2010;**16**:936-945.
12. Griffon-Etienne G, Boucher Y, Brekken C, Suit HD, Jain RK. Taxane-induced apoptosis decompresses blood vessels and lowers interstitial fluid pressure in solid tumors: clinical implications. *Cancer Res* 1999;**59**:3776-3782.
13. Vlahovic G, Ponce AM, Rabbani Z, Salahuddin FK, Zgonjanin L, Spasojevic I, et al. Treatment with imatinib improves drug delivery and efficacy in NSCLC xenografts. *Br J Cancer* 2007;**97**:735-740.
14. Tufto I, Rofstad EK. Interstitial fluid pressure, fraction of necrotic tumor tissue, and tumor cell density in human melanoma xenografts. *Acta Oncol* 1998;**37**:291-297.
15. Song CW, Kim MS, Cho LC, Dusenbery K, Sperduto PW. Radiobiological basis of SBRT and SRS. *Int J Clin Oncol* 2014;**19**:570-578.
16. Park HJ, Griffin RJ, Hui S, Levitt SH, Song CW. Radiation-induced vascular damage in tumors: implications of vascular damage in ablative hypofractionated radiotherapy (SBRT and SRS). *Radiat Res* 2012;**177**:311-327.

17. Lovey J, Lukits J, Remenar E, Koronczay K, Kasler M, Nemeth G, et al. Antiangiogenic effects of radiotherapy but not initial microvessel density predict survival in inoperable oropharyngeal squamous cell carcinoma. *Strahlenther Onkol* 2006;**182**:149-156.
18. Harrington KJ, Rowlinson-Busza G, Uster PS, Vile RG, Peters AM, Stewart JS. Single-fraction irradiation has no effect on uptake of radiolabeled pegylated liposomes in a tumor xenograft model. *Int J Radiat Oncol Biol Phys* 2001;**49**:1141-1148.
19. Henriksen JR, Petersen AL, Hansen AE, Frankaer CG, Harris P, Elema DR, et al. Remote loading of (64)Cu(2+) into liposomes without the use of ion transport enhancers. *ACS Appl Mater Interfaces* 2015;**7**:22796-22806.
20. Reyes-Aldasoro CC, Griffiths MK, Savas D, Tozer GM. CAIMAN: an online algorithm repository for cancer image analysis. *Comput Methods Programs Biomed* 2011;**103**:97-103.
21. Fliedner FP, Hansen AE, Jorgensen JT, Kjaer A. The use of Matrigel has no influence on tumor development or PET imaging in FaDu human head and neck cancer xenografts. *BMC Med Imaging* 2016;**16**:5.
22. Znati CA, Rosenstein M, McKee TD, Brown E, Turner D, Bloomer WD, et al. Irradiation reduces interstitial fluid transport and increases the collagen content in tumors. *Clin Cancer Res* 2003;**9**:5508-5513.
23. Koukourakis MI, Koukouraki S, Giatromanolaki A, Archimandritis SC, Skarlatos J, Beroukas K, et al. Liposomal doxorubicin and conventionally fractionated radiotherapy in the treatment of locally advanced non-small-cell lung cancer and head and neck cancer. *J Clin Oncol* 1999;**17**:3512-3521.
24. Stapleton S, Milosevic M, Tannock IF, Allen C, Jaffray DA. The intratumoral relationship between microcirculation, interstitial fluid pressure and liposome accumulation. *J Control Release* 2015;**211**:163-170.
25. Stapleton S, Allen C, Pintilie M, Jaffray DA. Tumor perfusion imaging predicts the intra-tumoral accumulation of liposomes. *J Control Release* 2013;**172**:351-357.
26. Stapleton S, Jaffray D, Milosevic M. Radiation effects on the tumor microenvironment: implications for nanomedicine delivery. *Adv Drug Deliv Rev* 2017;**109**:119-30.
27. Hagtvet E, Roe K, Olsen DR. Liposomal doxorubicin improves radiotherapy response in hypoxic prostate cancer xenografts. *Radiat Oncol* 2011;**6**:135.
28. Harrington KJ, Rowlinson-Busza G, Syrigos KN, Vile RG, Uster PS, Peters AM, et al. Pegylated liposome-encapsulated doxorubicin and cisplatin enhance the effect of radiotherapy in a tumor xenograft model. *Clin Cancer Res* 2000;**6**:4939-4949.